Hindawi Publishing Corporation
Journal of Nanomaterials
Volume 2013, Article ID 747963, 10 pages
http://dx.doi.org/10.1155/2013/747963

Research Article

Preparation, Characterization, Thermal, and Flame-Retardant Properties of Green Silicon-Containing Epoxy/Functionalized Graphene Nanosheets Composites

Ming-Yuan Shen,[1,2] Chen-Feng Kuan,[3] Hsu-Chiang Kuan,[3] Chia-Hsun Chen,[4] Jia-Hong Wang,[5] Ming-Chuen Yip,[1] and Chin-Lung Chiang[5]

[1] *Department of Power Mechanical Engineering, National Tsing Hua University, Hsinchu 300, Taiwan*
[2] *Plastic Industry Development Center, Taichung 407, Taiwan*
[3] *Department of Computer Application Engineering, Far East University, Tainan 744, Taiwan*
[4] *Department of Material Science and Engineering, Far East University, Tainan 744, Taiwan*
[5] *Green Flame Retardant Material Research Laboratory, Department of Safety, Health and Environmental Engineering, Hung-Kuang University, Taichung 433, Taiwan*

Correspondence should be addressed to Chin-Lung Chiang; dragon@sunrise.hk.edu.tw

Received 4 January 2013; Revised 15 March 2013; Accepted 15 March 2013

Academic Editor: Christian Brosseau

In this investigation, silane was grafted onto the surface of graphene nanosheets (GNSs) through free radical reactions, to form Si-O-Et functional groups that can undergo the sol-gel reaction. To improve the compatibility between the polymer matrix and the fillers, epoxy monomer was modified using a silane coupling agent; then, the functionalized GNSs were added to the modified epoxy to improve the thermal stability and strengthen the flame-retardant character of the composites. High-resolution X-ray photoelectron spectrometry reveals that when the double bonds in VTES are grafted to the surfaces of GNSs. Solid-state 29Si nuclear magnetic resonance presents that the distribution of the signal associated with the T^3 structure is wide and significant, indicating that the functionalization reaction of the silicone in the modified epoxy and VTES-GNSs increases the network-like character of the structures. Thermal gravimetric analysis, the integral procedure decomposition temperature, and limiting oxygen index demonstrate that the GNSs composites that contained silicon had a higher thermal stability and stronger flame-retardant character than pure epoxy. The dynamic storage modulus of all of the m-GNSs containing composites was significantly higher than that of the control epoxy, and the modulus of the composites increased with the concentration of m-GNSs.

1. Introduction

Plastics are used in everyday life and have become indispensable. For example, polypropylene (PP), polyethylene (PE), and epoxy are extensively used because they are cheap and exhibit high plasticity. However, their disadvantage is their extreme flammability: they can be destroyed by even a small flame. Their involvement in accidental fires can put lives and property at stake. To prevent the occurrence of such hazardous risks, such plastics are modified to reduce their flammability. In the past, traditional halogenated flame retardants have been added to provide flame-retardant character. These retardants capture free radicals during combustion. Nevertheless, the process of combustion could be volatile, releasing harmful substances, such as dioxin and furan, which can be very harmful when inhaled. In recent years, international codes and regulations, such as WEEE (waste from electric and electronic equipment) and RoHS (restrictions of hazardous substances), have been established as awareness of these green issues has increased. Along these lines, a campaign for halogen-free products has been launched [1–7]. Hence, various halogen-free flame retardants

are being developed. They use nitrogen, phosphorus, silicon, intumescent flame retardants, and expandable graphite [8]. This study analyzes the addition of functionalized graphene nanosheets to the substrate. Graphene is becoming a popular subject of research. It is a flat monolayer of carbon atoms tightly packed into a two-dimensional (2D) honeycomb lattice [9]. It has uniquely physical, chemical, and mechanical properties such as high electron mobility (250,000 cm^2/Vs), high mechanical strength (>1060 GPa), high thermal conductivity (5000 $Wm^{-1} K^{-1}$), and high specific surface area (2600 $m^2 g^{-1}$). These properties make graphene the best polymer composite with extremely favorable polymer composite with the best mechanical, electrical, and thermal properties [10, 11]. Graphene has also been proven to improve the thermal properties and flame resistance when trace amounts of it are added thereto [12].

In this investigation, GNSs and epoxy were functionalized using a coupling agent to participate in place of sol-gel reactions to form compact networks that improve the compatibility between matrix and fillers at their interfaces. High-resolution X-ray photoelectron spectrometry (XPS) and solid-state ^{29}Si nuclear magnetic resonance spectroscopy (NMR) were utilized to characterize the grafting reaction between GNSs and silane and the structure of the composite material, respectively. Scanning electron microscopy (SEM) and transmission electron microscopy (TEM) were used to examine the morphology of the composite material. Thermal gravimetric analysis (TGA) was conducted, and integral procedure decomposition temperature (IPDT) and limiting oxygen index (LOI) were then used as metrics of thermal stability and flame-retardant character, respectively.

2. Experimental

2.1. Materials. Graphene nanosheets (GNSs) were purchased from Xiamen Knano Graphene Technology Co. Ltd, China. 3-Isocyanatopropyltriethoxysilane (IPTS), vinyltriethoxysilane (VTES), tetrahydrofuran (THF), triethylamine (TEA), and bezoyl peroxide (BPO) were purchased from ECHO Chemical Co. Ltd., Taiwan. Diglycidyl ether of bisphenol-A, DGEBA type epoxy, was kindly supplied by Nan-Ya Plastics Corporation, Taiwan. 4, 4′-Diaminodiphenylmethane (DDM) as a curing agent for epoxy was purchased from Sigma-Aldrich Co. Ltd., UK. Hydrochloric acid (HCl) as a catalyst for sol-gel reaction was purchased from Union Chemical Works Ltd., Taiwan.

2.2. Experiment Flowchart. Figure 1 shows the flowchart of the experiment.

2.3. Grafting Reaction between GNSs and VTES. One g of GNSs was placed into the solvent THF to implement ultrasonic bath for 90 minutes, so that the GNSs can become more dispersed without clustering in the solvent, which will then be filtered and placed into the oven to heat 4 hours in temperature of 80°C until dry. The GNSs is synthesized with VTES. First, the GNSs and VTES are mixed with weight ratio in 1:1 to adopt mechanical mixer for mixing, using BPO (VTES : BPO = 1 : 0.02 mol) as the initiator to stir for about 8 hours with temperature controlled at 80°C, so that the functionalization of GNSs and VTES can undergo the free radical reaction for grafting. GNSs containing functionalized siloxane groups will be filtered and dried to finish the processing of VTES-GNSs. The reaction scheme is shown in Figure 2(a).

2.4. Preparation for Epoxy/m-GNSs Composite Materials. Epoxy matrix was modified by IPTS, using TEA as a catalyst to speed up the reaction, so that the substrate epoxy contains functionalized silane with more compatibility with the aforementioned VTES-GNSs. The modified epoxy was synthesized as follows: 4 g IPTS (equivalent weight 247 g) was added into 10 g DGEBA type epoxy (equivalent weight 180 g) at 60°C, then it was stirred for 4 hours until the characteristic peak of NCO group disappeared. Adding 0.1 wt%, 0.5 wt%, 1 wt%, 5 wt%, and 10 wt% modified GNSs into the epoxy solution to carry out the hydrolysis-condensation reaction with the modified epoxy. The deionized water (DI water) and HCI as catalysis were added into the mixtures of epoxy and VTES-GNSs and stirred with magnet at 80°C for 8 hours, followed by adding DDM as curing agent until the solvent appears with viscous liquid. The mixture is then poured into the aluminum tray and placed in room temperature for 24 hours, and then is placed into the oven and heat from starting temperature of 80°C to 160°C. The finished product is epoxy/m-GNSs composite material, with its reaction formula shown in Figure 2(b).

2.5. Measurements. Fourier transform infrared spectroscopy (FT-IR, Perkin Elmer, Spectrum one 72930): the reaction solution is evenly coated on the KBr salt sheet and placed into the IR instrument. The changes during the reaction are tested and analyzed.

High-resolution X-ray photoelectron spectrometer (HR-XPS, ULVAC-PHI, Inc., Kanagawa-ken, Japan): the sample is crushed into powder, and the sample is then adhered to the aluminum sheet with small round holes, which is mainly used for detecting the sample surface as well as the element composition and distribution in vertical directions, in addition to implementing analysis on the links of element substances.

Field emission scanning electron microscope (FE-SEM, JEOL JSM-6700F, Japan): the sample undergoes gold or silver plating and photographed in a vacuumed instrument under high magnification.

Thermogravimetric analyzer (TGA, Perkin Elmer Pyris 1 TGA, USA): the required temperature rising rate is set up first, and the sample is placed into the platinum crucible, which is hung by the quartz hook with a weight of scale approximately between 5 and 10 mg, which is then placed into the furnace tube to implement the observation of decomposition curve analysis from room temperature to 800°C.

Limited oxygen index (LOI, ATLAS Fire Science Products, USA): the sample is crushed into granites of powder and placed into the crucible, which is then tested with the nature

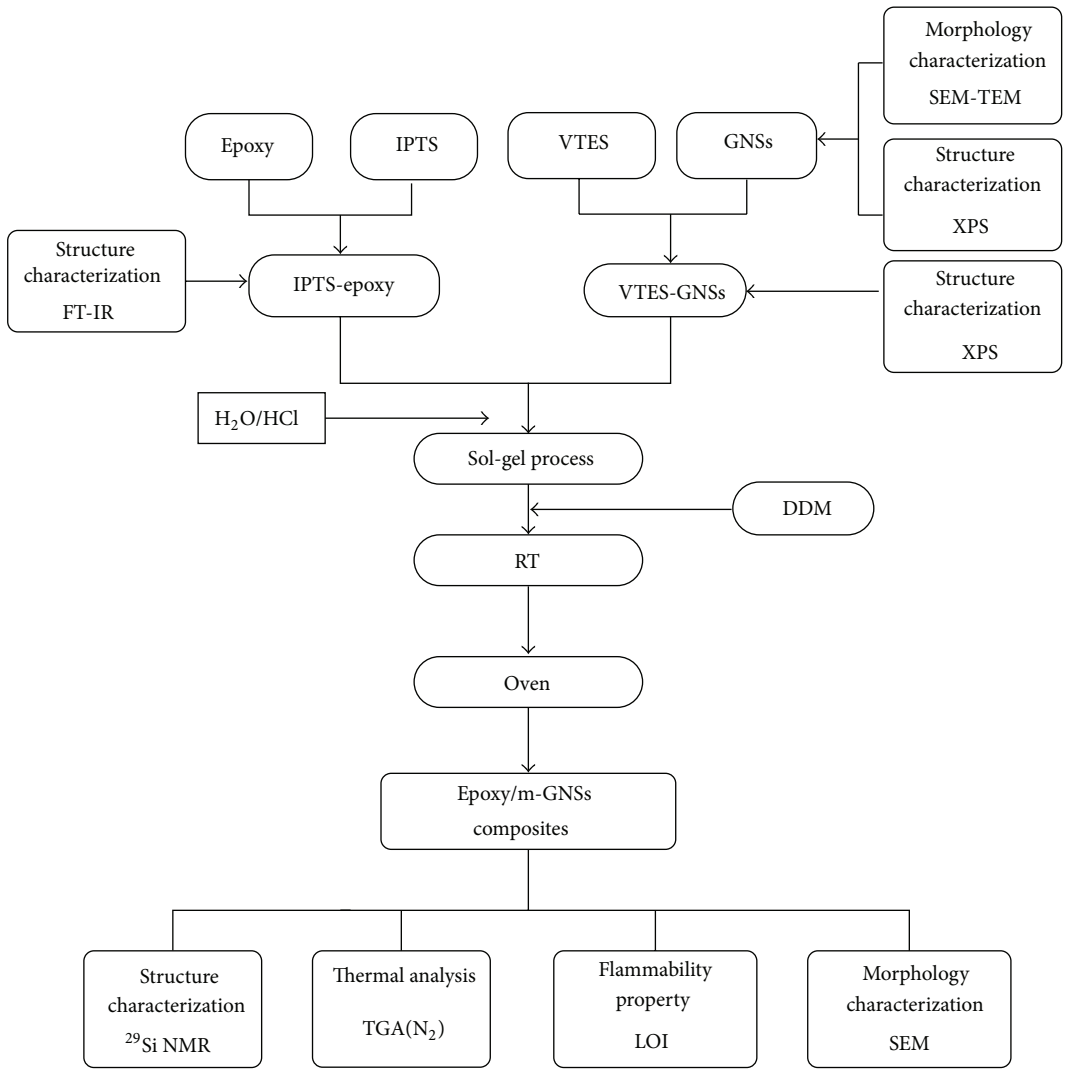

Figure 1: Experimental flow chart of composite.

of flame retardancy after moderating the nitrogen and oxygen concentration in the instrument.

Solid-state ^{29}Si nuclear magnetic resonance spectroscopy (NMR, Bruker DSX400WB): the sample is placed into powder with approximate weight about 0.2~0.3 g, which is then tested and placed into the instrument for nuclear magnetic resonance (NMR).

Transmission electron microscopy (TEM, Hitachi H-7100): the sample was crushed into powder, placed into a small bottle, added with ethanol as solvent, and moved before testing. The high-energy electron beam (approximately 100 keV~1 MeV) was applied to a thin-layer sample with transmission thickness under 100 nm.

The morphology of the fractured surface of the composites was studied under a scanning electron microscope (SEM) (JEOL JSM 840A, Japan). The distributions of Si atoms in the char were obtained from SEM EDX mapping (JEOL JSM 840A, Japan).

2.6. Reaction Scheme. Figure 2 shows the reaction scheme of the VTES-GNSs and epoxy/VTES-GNSs composites.

3. Results and Discussion

3.1. Characterization of Modification of Epoxy Matrix. To improve the compatibility of an epoxy matrix with the fillers, epoxy resin was modified by IPTS, using TEA as a catalyst, in a reaction between the –OH of epoxy and the –NCO of IPTS to form IPTS-epoxy, as displayed in Figure 3. Figure 3(a) demonstrates that, before modification, IPTS-epoxy mixtures exhibited a significant characteristic peak associated with the –NCO group of IPTS at 2270 cm^{-1} [13]. Figure 3(b) reveals clearly that the characteristic peak at 2270 cm^{-1} disappeared upon 8 hours of chemical reaction, indicating that IPTS can be successfully grafted on the epoxy backbones. Following the modification, epoxy resin had Si–O–Et functional groups, which underwent the sol-gel reaction with VTES-GNSs to

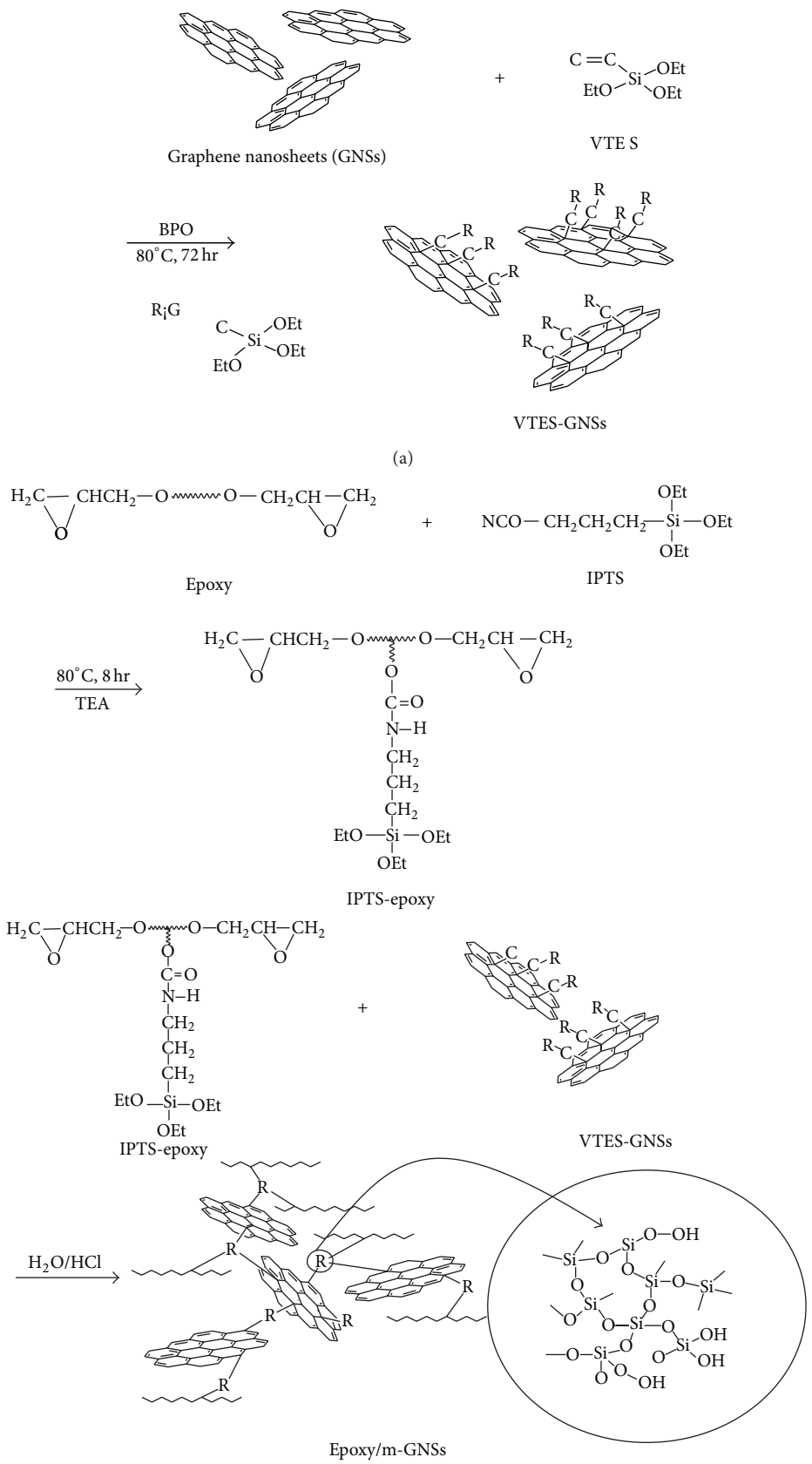

Figure 2: Reaction schemes of (a) VTES-GNSs and (b) epoxy/m-GNSs composites.

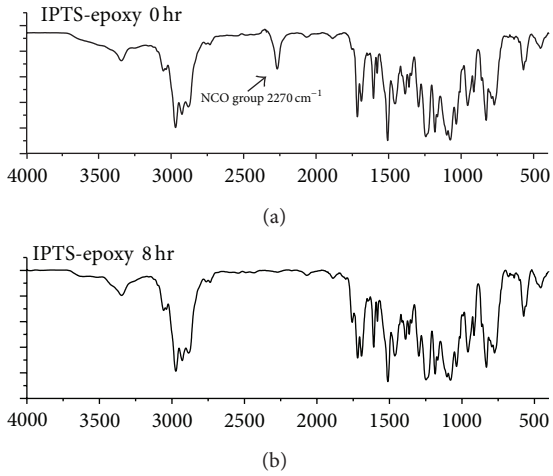

FIGURE 3: FT-IR spectra of IPTS-epoxy mixtures (a) initial time t = 0 and (b) after 8 hours.

connect the interfaces between the epoxy matrix and the GNSs.

3.2. Characterization of Grafting Reaction of VTES on the Surfaces of GNSs. XPS was utilized to elucidate the grafting reaction of VTES onto the surfaces of GNSs. Figure 4 presents the wide scanning and narrow scanning C 1s XPS spectra of GNSs and VTES-GNSs. Before modification, the most important signal in the wide-scan XPS spectrum was that of the GNSs, which did not contain silicon, as displayed in Figure 4(a). Figure 4(b) indicates that silane yielded Si2s and Si2p peaks at binding energies of 152.18 and 103.56 eV [14, 15], respectively, indicating that the double bond of VTES was successfully grafted on the surfaces of the GNSs. Additionally, the narrow scan C1s spectrum of GNSs in Figure 4(c) includes typical C–C and C=C peaks at binding energies of 284.4 eV and 284.8 eV, respectively [16, 17]. The multiple oxygen-containing functional groups on GNSs were responsible for the C–O and C=O characteristics peaks [18] between 285.7 eV and 287.4 eV, probably because GNSs underwent oxidation and restored into GNSs by thermal shock, while some residual oxygen-containing functional groups remained on its top [19]. The narrow-scan XPS in Figure 4(d) reveals peaks associated with modified GNSs: the new C–Si peak is observed at 284.2 eV while the C=C signal, substantially smaller, is observed at 284.8 eV site. These findings reveal that, when the double bonds in VTES are grafted to the surfaces of GNSs, signals associated with C–Si bonds are observed and the characteristics peaks of the double bonds are greatly weakened.

Figure 5 displays the TEM image of the surfaces of VTES-GNSs, which reveals layers of stacked graphene nanosheets. The total thickness of these sheets is less than 100 nm, revealing the irregular penetration of light. This image is that of graphene nanosheets [20]. The black dots, which look like clouds, indicate that GNSs were modified by the VTES and that the silane was successfully grafted to the surfaces of the GNSs.

3.3. Characterization for Preparation of Composites. Solid-state ^{29}Si-NMR is used to monitor the hydrolysis-condensation reaction between modified epoxy and functionalized graphene nanosheets (VTES-GNSs) through the sol-gel reaction. In condensed siloxane species for VTES and IPTS, silicon atoms through that have mono-, di-, trisubstituted siloxane bonds are designated as T^1, T^2, and T^3, respectively. The chemical shifts associated with T^1, T^2, and T^3 are −45, −58, and −65 ppm, respectively, whose values are consistent with those in the literature [21]. The peaks of the curve in Figure 6 reveal that the distribution of the signal associated with the T^3 structure is wide and significant, indicating that the functionalization reaction of the silicone in the modified epoxy and VTES-GNSs increases the network-like character of the structures. The network structures promote the thermal stability of hybrids.

SEM is used herein to observe the morphology of composite materials. The thickness, size, and stacking states of the graphene nanosheets prove that GNSs are nanoscale structures. Figure 7(a) shows that at a magnification of 30 K x, the thickness of GNSs is significantly less than 100 nm, proving that the structures are graphene nanosheets. Next, the dispersion of VTES-GNSs in polymer substrate was determined from the dissection diagram of epoxy/m-GNSs 1% composite materials, which was magnified 2,000 times in Figure 7(b). The modified graphene nanosheets have been successfully processed in the substrate, forming the nanocomposite material. The epoxy/m-GNSs 1% composite material underwent combustion and clearly revealed the formation of a dense network structure that uniformly covered the substrate from the surface of the substrate, as displayed in Figure 7(c), facilitating char layer protection of the substrate by a char layer during combustion [22]. Figure 8 presents the EDS of epoxy/m-GNSs 1% composites following combustion. The flame retardant that contains silicon decomposes into silicon dioxide (SiO_2) when it is heated in an atmosphere of air, forming an inorganic protective layer on the substrate, isolating it from the source of the fire, and inhibiting exchanges of mass and energy.

3.4. Thermal Properties of Composites. Various concentrations of composite materials were tested using a thermogravimetric analyzer in an atmosphere of nitrogen. They were heated at 20°C/min from room temperature to 800°C, and TGA and DTG curves were obtained. Figure 8 plots the TGA and DTG curves, and Table 1 presents the thermal and flame-retardant properties of epoxy/m-GNSs composites. Table 1 and Figure 9(a) reveal that the char yield of epoxy/m-GNSs increased from 13.8 wt% (pure epoxy) to 26.2 wt% (epoxy/m-GNSs 10), indicating an effective improvement of 12.4 wt%. This finding demonstrates that m-GNSs improve the thermal stability of epoxy resin at high temperature. Adding trace of VTES-GNSs (0.1 wt%) can significantly improve thermal properties. Si and GNSs are speculated to prevent volatility and adhesion to the surface of the substrate during combustion, making GNSs containing silicon compatible with the grafted substrate that contains silicon, such that a SiO_2 network structure is formed by the hydrolysis-condensation

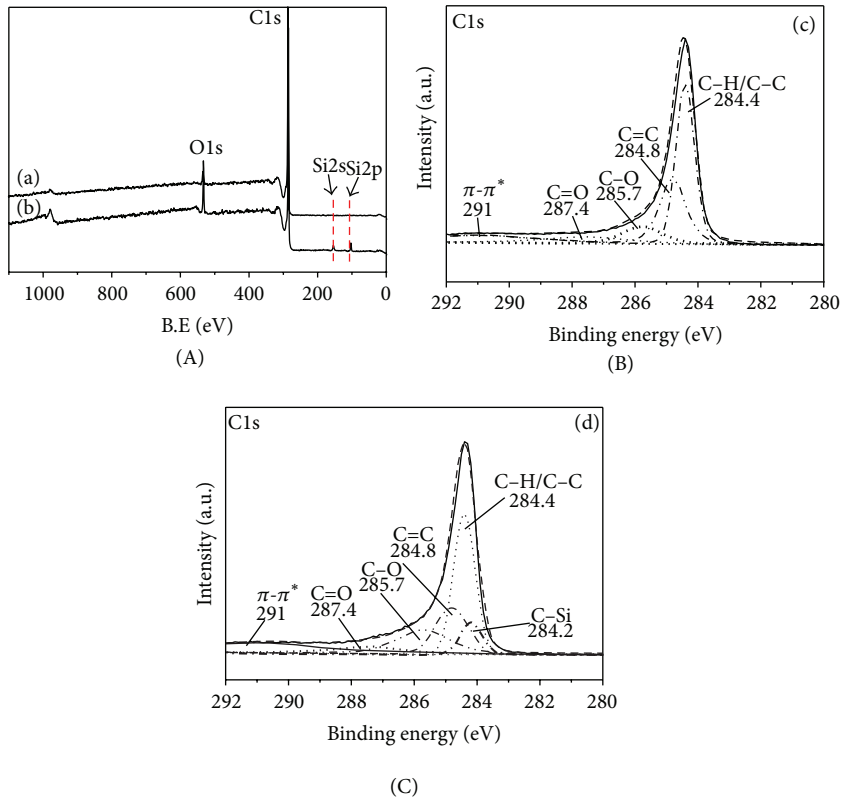

Figure 4: High-resolution XPS spectra of the surface of (a) wide scan of GNSs, (b) wide scan of VTES-GNSs, (c) narrow scan of GNSs, and (d) narrow scan of VTES-GNSs for C 1s.

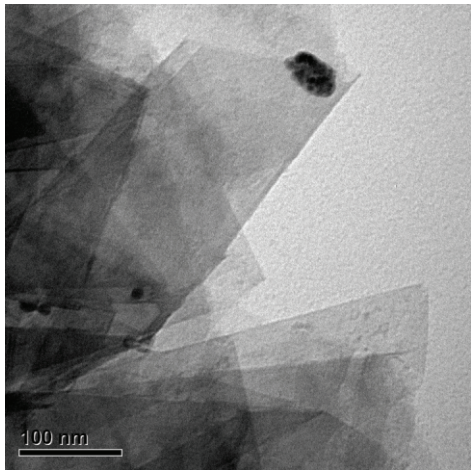

Figure 5: The TEM microphotographs of VTES-GNSs.

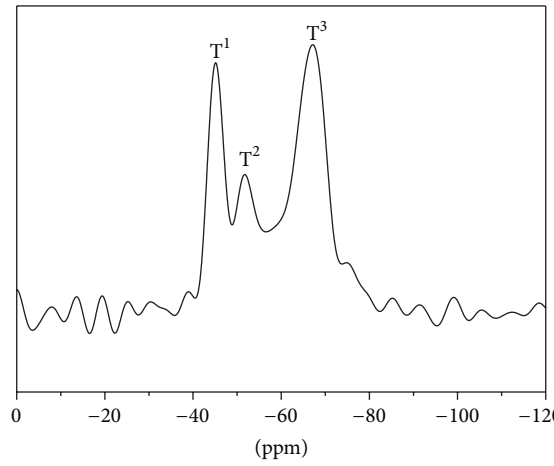

Figure 6: Solid-state ^{29}Si-NMR of epoxy/m-GNSs composites.

process. This structure is a protective layer of char. The char yield increases with the filler concentration [23–25].

Figure 9(b) shows that T_{max}, which is the temperature at the maximum rate of thermal degradation, increased from 402.6°C (pure epoxy) to 426.7°C (epoxy/m-GNSs 10), indicating that decomposition was postponed by an increase in the thermal degradation temperature. The maximum rate of thermal degradation decreased from −26.8%/°C (pure epoxy) to −12.7%/°C (epoxy/m-GNSs 10), suggesting an effective slowing of decomposition while the continuation of thermal decomposition is effectively prevented, so that the polymer materials do not instantly combust and collapse.

The integral procedural decomposition temperature (IPDT), proposed by Doyle [26], has been associated with the volatility of polymeric materials and used as an estimate of the

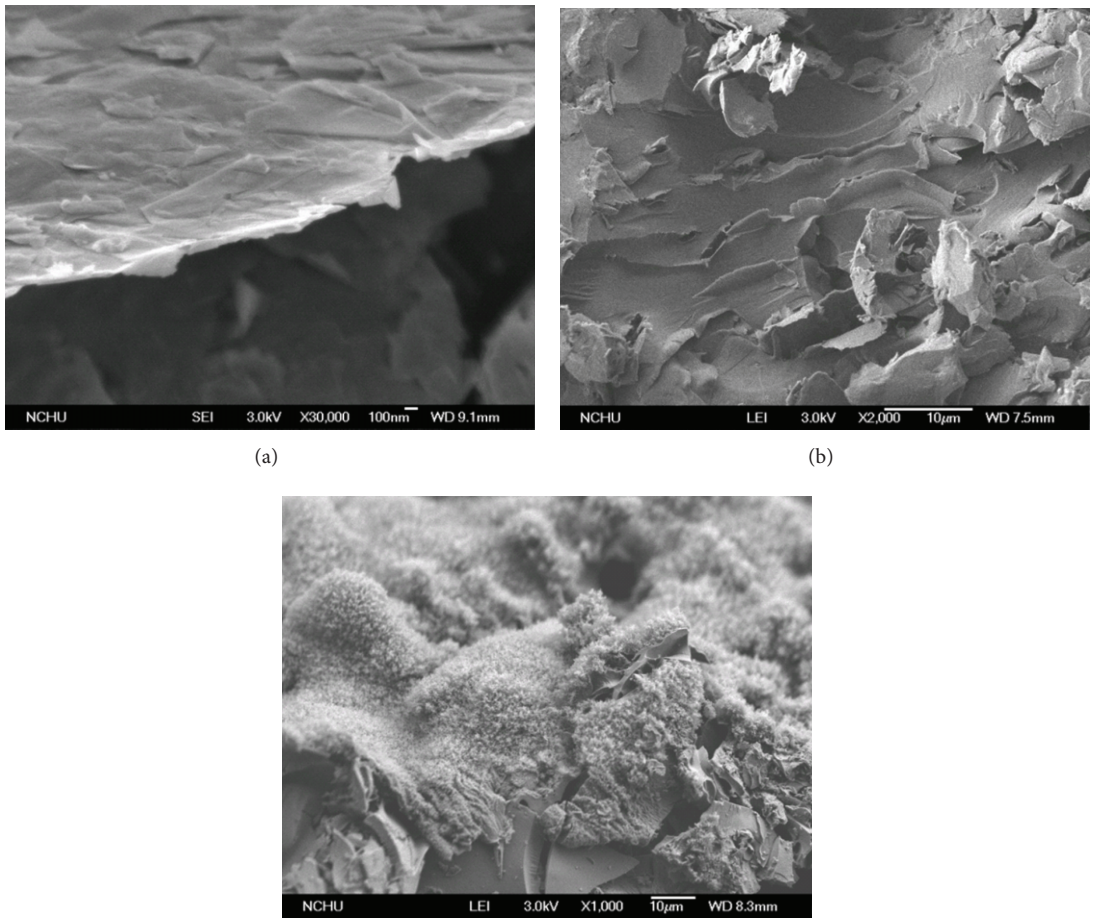

(a) (b) (c)

Figure 7: The SEM microphotographs of (a) GNSs (×30 k), (b) epoxy/m-GNSs 1% composites (×2 k) before combustion, and (c) epoxy/m-GNSs 1% composites (×1 k) after combustion.

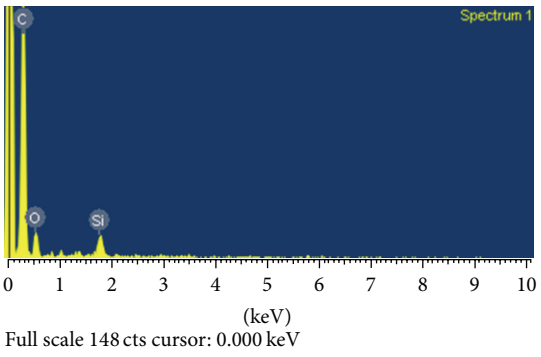

Figure 8: EDS of epoxy/m-GNSs 1% composites after combustion.

inherent thermal stability of polymeric materials. IPDT is as given by Figure 10 and

$$T_i = (\text{experimental temperature}, 30^\circ\text{C})$$

$$T_f = (\text{final experimental temperature}, 800^\circ\text{C})$$

$$A^* = \frac{(S_1 + S_2)}{(S_1 + S_2 + S_3)}$$

Table 1: Thermal and flame-retardant properties of epoxy/m-GNSs composites.

Sample no.	T_{max} (°C)	Maximum thermal degradation rate (wt%/°C)	IPDT (°C)	Char (wt%)	LOI
Pure epoxy	402	−26.8	588	13.8	21
Epoxy/m-GNSs 0.1	426	−18.1	733	20.9	24
Epoxy/m-GNSs 0.5	425	−17.2	749	21.4	25
Epoxy/m-GNSs 1	426	−15.9	797	24.0	26
Epoxy/m-GNSs 5	415	−15.0	834	25.3	26
Epoxy/m-GNSs 10	427	−12.5	853	26.2	27

$$K^* = \frac{(S_1 + S_2)}{S_1}$$

$$\text{IPDT} = A^* \times K^* \times (T_f - T_i) + T_i. \quad (1)$$

Table 1 data, 733°C (epoxy/m-GNSs 0.1%), 749°C (epoxy/m-GNSs 0.5%), 797°C (epoxy/m-GNSs 1%), 834°C

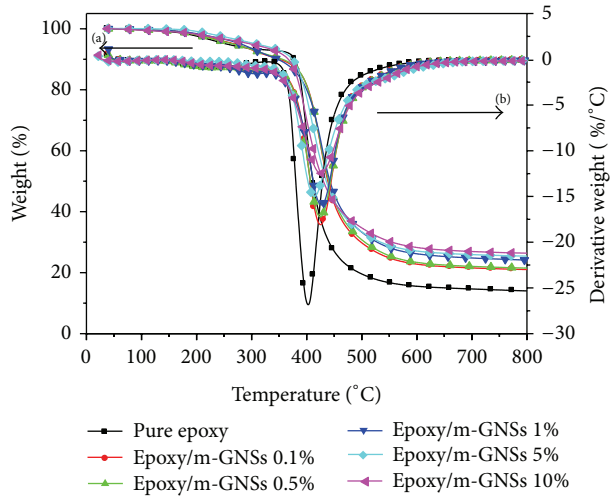

Figure 9: (a) TGA curves, (b) DTG curves.

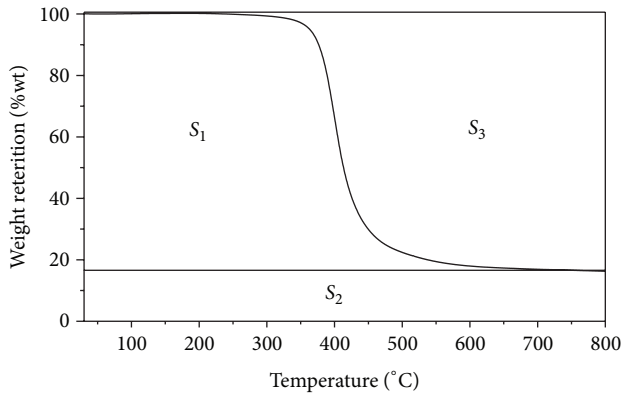

Figure 10: Schematic representation of S_1, S_2, and S_3 for A^* and K^*.

(epoxy/m-GNSs 5%), and 853°C (epoxy/m-GNSs 10%), were all higher than 588°C (pure epoxy). This noticeable effect in the thermal properties is attributed to the barrier effects of graphene sheets. Specially, only few amounts of m-GNSs (0.1 wt% m-GNSs) were added into polymer matrix, it will result in the improvement on IPDT, which is from 588°C to 733°C. The IPDT values significantly improved as the concentration was increased. The thermal stability of hybrids increased with the total inorganic content. The inorganic components improve the thermal stability of composites.

3.5. Flame-Retardant Property of Composites. LOI is used mainly as a measure of the flame retardancy of materials in a confined space. LOI is defined as follows, where $[O_2]$ and $[N_2]$ are set flow rates (mL/sec):

$$\text{LOI} = \frac{[O_2]}{[O_2] + [N_2]} \times 100. \quad (2)$$

According to (2), LOI is less than 22, indicating that the sample is flammable. If LOI of the sample is more than 22 and equal or less than 25, the material is self-extinguishing.

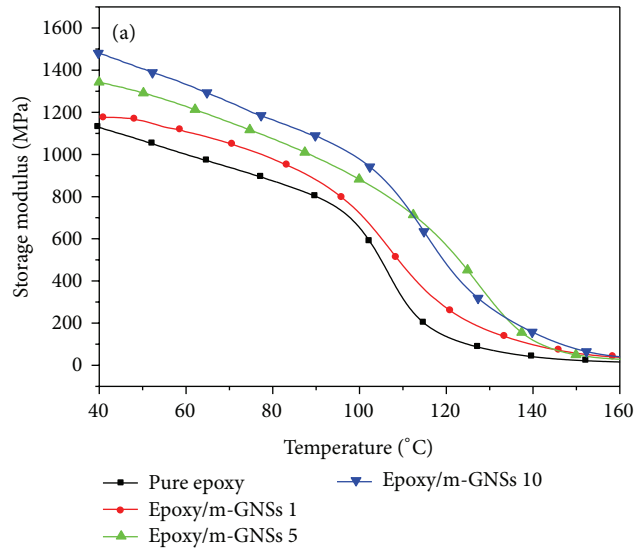

Figure 11: Storage modulus as a function of temperature for the control epoxy and for the composites.

LOI is more than 26, and the material reaches flame retardant level. The materials have higher LOI values, meaning that they possess better flame retardant property.

From Table 1, the LOI of pure epoxy is only 21, so it is highly flammable. The LOI of epoxy/m-GNS 10 wt% composites is 27, indicating that it is flame retardant level. The LOI of the composites, and therefore the flame retardancy, increase with VTES-GNS content. Adding a trace amount of VTES-GNSs (0.1 wt%) to epoxy clearly improves its flame retardancy. The graphene promotes the formation of compact char layers in condensed phase during combustion in polymer matrix. Furthermore, the char reinforced by graphene sheets effectively prevents the polymer thermal decomposition products into the flame zone and that of the oxygen into the underlying of polymer matrix [27].

3.6. Dynamic Mechanical Properties. Dynamic storage modulus is shown in Figure 11 as plots of storage modulus versus temperature for the control epoxy and for the composites. It is interesting to note that in the glass state, the dynamic storage modulus of all of the m-GNSs containing composites was significantly higher than that of the control epoxy, and the modulus increased with the concentration of m-GNSs. In the composites systems, the m-GNSs were homogeneously dispersed in the epoxy matrices due to the modification of the surfaces of GNSs, and thus the increased modulus could be attributed to the reinforcing effect of m-GNSs on the epoxy matrix.

4. Conclusion

Epoxy nanocomposites that contained graphene nanosheets and silicon were prepared using the sol-gel method. XPS provides clear evidence that VTES was grafted onto the surfaces of GNSs. The NMR spectrum thereof established the formation of networks between epoxy matrix and GNSs via

a sol-gel reaction. TGA and LOI indicate that the composites had better thermal stability and flame retardancy than pure epoxy, and so could effectively reduce the occurrence of fire.

Acknowledgments

The authors would like to thank the National Science Council, Taiwan, for financially supporting this research under Contract no. NSC NSC-101-2628-E-241-002. Ted Knoy is appreciated for his editorial assistance.

References

[1] F. Barontini and V. Cozzani, "Formation of hydrogen bromide and organobrominated compounds in the thermal degradation of electronic boards," *Journal of Analytical and Applied Pyrolysis*, vol. 77, no. 1, pp. 41–55, 2006.

[2] A. K. Sen, B. Mukherjee, A. S. Bhattacharya, L. K. Sanghi, P. P. De, and A. K. Bhowmick, "Preparation and characterization of low-halogen and nonhalogen fire-resistant low-smoke (FRLS) cable sheathing compound from blends of functionalized polyolefins and PVC," *Journal of Applied Polymer Science*, vol. 43, no. 9, pp. 1673–1684, 1991.

[3] M. J. Chen, Z. B. Shao, X. L. Wang, L. Chen, and Y. Z. Wang, "Halogen-free flame-retardant flexible polyurethane foam with a novel nitrogen-phosphorus flame retardant," *Industrial and Engineering Chemistry Research*, vol. 51, no. 29, pp. 9769–9776, 2012.

[4] L. Du, G. Xu, Y. Zhang, J. Qian, and J. Chen, "Synthesis and properties of a novel intumescent flame retardant (IFR) and its application in halogen-free flame retardant ethylene propylene diene terpolymer (EPDM)," *Polymer-Plastics Technology and Engineering*, vol. 50, no. 4, pp. 372–378, 2011.

[5] K. C. Tsai, C. F. Kuan, C. H. Chen et al., "Study on thermal degradation and flame retardant property of halogen-free polypropylene composites using XPS and cone calorimeter," *Journal of Applied Polymer Science*, vol. 127, no. 2, pp. 1084–1091, 2013.

[6] T. M. D. Nguyen, S. Chang, B. Condon, M. Uchimiya, and C. Fortier, "Development of an environmentally friendly halogen-free phosphorus-nitrogen bond flame retardant for cotton fabrics," *Polymers for Advanced Technologies*, vol. 23, no. 12, pp. 1555–1563, 2012.

[7] Y. Bai, X. Wang, and D. Wu, "Novel cyclolinear cyclotriphosphazene-linked epoxy resin for halogen-free fire resistance: synthesis, characterization, and flammability characteristics," *Industrial and Engineering Chemistry Research*, vol. 51, no. 46, pp. 15064–15074, 2012.

[8] Z. Wang, E. Han, and W. Ke, "Influence of expandable graphite on fire resistance and water resistance of flame-retardant coatings," *Corrosion Science*, vol. 49, no. 5, pp. 2237–2253, 2007.

[9] J. C. Slonczewski and P. R. Weiss, "Band structure of graphite," *Physical Review*, vol. 109, no. 2, pp. 272–279, 1958.

[10] S. Stankovich, D. A. Dikin, G. H. B. Dommett et al., "Graphene-based composite materials," *Nature*, vol. 442, no. 7100, pp. 282–286, 2006.

[11] A. Yu, P. Ramesh, M. E. Itkis, E. Bekyarova, and R. C. Haddon, "Graphite nanoplatelet-epoxy composite thermal interface materials," *Journal of Physical Chemistry C*, vol. 111, no. 21, pp. 7565–7569, 2007.

[12] M. C. Hsiao, S. H. Liao, M. Y. Yen et al., "Preparation of covalently functionalized graphene using residual oxygen-containing functional groups," *ACS Applied Materials & Interfaces*, vol. 2, no. 11, pp. 3092–3099, 2010.

[13] W. Wei, H. Zhang, S. Guan, Z. Jiang, and X. Yue, "Preparation and characterization of transparent polyarylethers-silica hybrid membranes with covalently connected phases," *Polymer*, vol. 53, pp. 5002–5009, 2012.

[14] S. Ganguli, A. K. Roy, and D. P. Anderson, "Improved thermal conductivity for chemically functionalized exfoliated graphite/epoxy composites," *Carbon*, vol. 46, no. 5, pp. 806–817, 2008.

[15] C. Perruchot, M. A. Khan, A. Kamitsi et al., "XPS characterisation of core-shell silica-polymer composite particles synthesised by atom transfer radical polymerisation in aqueous media," *European Polymer Journal*, vol. 40, no. 9, pp. 2129–2141, 2004.

[16] T. I. T. Okpalugo, P. Papakonstantiou, H. Murphy, J. Mclaughin, and N. M. D. Brown, "High resolution XPS characterization of chemical functionalized MECNT and SWCNT," *Carbon*, vol. 43, pp. 153–161, 2005.

[17] Z. X. Zhang, Y. D. Huang, T. Y. Wang, and L. Liu, "Influence of fibre surface oxidation-reduction followed by silsesquioxane coating treatment on interfacial mechanical properties of carbon fibre/polyarylacetylene composites," *Composites A*, vol. 38, no. 3, pp. 936–944, 2007.

[18] S. Sharma, A. Ganguly, P. Papakonstantinou et al., "Rapid microwave synthesis of CO tolerant reduced graphene oxide-supported platinum electrocatalysts for oxidation of methanol," *The Journal of Physical Chemistry C*, vol. 114, no. 45, pp. 19459–19466, 2010.

[19] G. Wang, X. Shen, B. Wang, J. Yao, and J. Park, "Synthesis and characterisation of hydrophilic and organophilic graphene nanosheets," *Carbon*, vol. 47, no. 5, pp. 1359–1364, 2009.

[20] T. A. Phama, J. S. Kimb, J. S. Kima, and Y. T. Jeonga, "One-step reduction of graphene oxide with L-glutathione," *Colloids and Surfaces A*, vol. 384, no. 1–3, pp. 543–548, 2011.

[21] T. M. Lee, C. C. M. Ma, C. W. Hsu, and H. L. Wu, "Effect of molecular structures and mobility on the thermal and dynamical mechanical properties of thermally cured epoxy-bridged polyorganosiloxanes," *Polymer*, vol. 46, no. 19, pp. 8286–8296, 2005.

[22] S. Hamdani, C. Longuet, D. Perrin, J. M. Lopez-cuesta, and F. Ganachaud, "Flame retardancy of silicone-based materials," *Polymer Degradation and Stability*, vol. 94, no. 4, pp. 465–495, 2009.

[23] Y. Y. Yu, C. Y. Chen, and W. C. Chen, "Synthesis and characterization of organic-inorganic hybrid thin films from poly(acrylic) and monodispersed colloidal silica," *Polymer*, vol. 44, no. 3, pp. 593–601, 2003.

[24] J. Xu, W. Shi, M. Gong, F. Yu, and L. Yan, "Preparation of poly(methyl methacrylate-co-maleic anhydride)/SiO_2-TiO_2 hybrid materials and their thermo- And photodegradation behaviors," *Journal of Applied Polymer Science*, vol. 97, no. 4, pp. 1714–1724, 2005.

[25] J. Macan, I. Brnardić, S. Orlić, H. Ivanković, and M. Ivanković, "Thermal degradation of epoxy—Silica organic—inorganic hybrid materials," *Polymer Degradation and Stability*, vol. 91, no. 1, pp. 122–127, 2006.

[26] C. D. Doyle, "Estimating thermal stability of experimental polymers by empirical thermogravimetric analysis," *Analytical Chemistry*, vol. 33, no. 1, pp. 77–79, 1961.

[27] G. Huang, H. Liang, Y. Wang, X. Wang, J. Gao, and Z. Fei, "Combination effect of melamine polyphosphate and graphene on flame retardant properties of poly(vinyl alcohol)," *Materials Chemistry and Physics*, vol. 132, pp. 520–528, 2012.